Microsyst Technol (2018) 24:2287–2294
https://doi.org/10.1007/s00542-017-3635-y

TECHNICAL PAPER

# Electrodeposition of Si–DLC nanocomposite film and its electronic application

**Necati Basman[1] · Rukiye Uzun[1] · Ebru Gocer[2] · Emin Bacaksiz[3] · Ugur Kolemen[2]**

Received: 28 July 2017 / Accepted: 13 November 2017 / Published online: 17 November 2017
© Springer-Verlag GmbH Germany, part of Springer Nature 2017

**Abstract** In this study, a silicon doped diamond-like carbon (DLC) nanocomposite film was deposited electrochemically and it was used to fabricate an Ag/Si–DLC/*p*-Si metal–interlayer–semiconductor (MIS) Schottky diode. Methanol ($CH_3OH$) was used as carbon and tetraethoxysilane ($Si(OC_2H_5)_4$) as Si source, respectively. Morphology of the film was observed by scanning electron microscopy and continuous surface with numerous lumps spread randomly was observed. Structural and chemical composition analyses of the film were carried out by Raman and X-ray photoelectron spectroscopy. Typical D and G bands of DLC films were not observed in the Raman spectrum due to abundance of Si–C bonds. Silicon incorporation promoted the film deposition and increased $sp^3$ bonds in the film. Current–Voltage (*I–V*) measurement was conducted to obtain parameters of the MIS diode. The diode exhibited a good rectifier behavior with $\sim 10^3$ rectification ratio. In the forward bias semi-logarithmic *I–V* plot, two linear regions with different slopes were observed. Such behavior was modelled by two parallel diodes and attributed to different conduction mechanism. The main electrical parameters, such as barrier height, ideality factor and series resistance were calculated by *I–V* and Cheung–Cheung methods. The Si–DLC nanocomposite film acted as barrier height modifier in the MIS diode.

✉ Necati Basman
nbasman@gmail.com

[1] Department of Electrical and Electronics Engineering, Bulent Ecevit University, Zonguldak, Turkey

[2] Department of Physics, Gaziosmanpasa University, Tokat, Turkey

[3] Deparment of Physics, Karadeniz Technical University, Trabzon, Turkey

## 1 Introduction

Diamond-like carbon (DLC) films are defined as amorphous carbon materials made up of random networks of $sp^2$ and $sp^3$ hybrid bonds (Robertson 2002; Li et al. 2009). These films have properties similar to those of diamond to a certain extent, such as high hardness with high wear resistance, high chemical inertness, high dielectric strength and high resistivity (Yan et al. 2004a; Wan et al. 2010; Nery et al. 2010; Tao et al. 2011; Chaus et al. 2014; Zeng et al. 2014). These extraordinary properties make them the most studied coating materials (Erdemir and Donnet 2006). An important part of the studies are conducted to explore the doping effect of different elements on the physical, mechanical and tribological properties of the films. It has been shown that doping elements provide remarkable improvements in the properties and functions of the films, such as, low friction coefficients, low abrasive wear rates, good adhesion to metal substrates, high hardness, the increment of conductivity and better optical properties (Papakonstantinou et al. 2002; Franta et al. 2003; Guerino et al. 2003; Huang et al. 2006; Choi et al. 2007; Caschera et al. 2011; Ahmed et al. 2009; Wang et al. 2010). Among the additive elements, Si is one of the most studied elements, as it solves some of the major disadvantages of pure DLC coatings, such as surface roughness, internal stress, friction coefficient and adhesion strength (Papakonstantinou et al. 2002; Franta et al. 2003; Kima et al. 2005; Choi et al. 2007; Laurikaitienė et al. 2008; Yi et al. 2009). In all of the Si doping studies, the DLC films were deposited by using chemical vapor deposition (CVD) or physical vapor deposition (PVD) techniques which are effortful. In contrast to these techniques, electrodeposition is an easy method which provide advantages of large area depositions, low deposition temperatures, low cost apparatus

(Zhang et al. 2008; Basman et al. 2015). Yan et al. (2004b) were the only group that deposited $SiO_2$ doped DLC film by using of the electrolysis of methanol-dimethylethoxy-disilane (DDS) solution.

Electronic applications of DLC materials have also been attracting attention due to their superior properties and many studies have been carried out. Most of these studies are related to their cold cathode field emitters, a-C/c-Si heterostructures, electrical conductivity, solar cells and dielectric strength and how their electronic properties are changed by doping an element (Silva et al. 1999; Milne 2003; Bhattacharyya and Silva 2007; Gao et al. 2007; Wang et al. 2010; Li et al. 2009; Katsuno et al. 2006; Meškinis et al. 2014). It has been reported that dielectric strength, resistivity and band gap could be changed by varying the proportion of $sp^3$ and $sp^2$ hybridized carbon bonds upon doping. In spite of the aforementioned improving effect of Si doping, according to our best knowledge, electronic applications of Si doped DLC films have not been studied yet.

Metal/interlayer/semiconductor (MIS) contacts have been investigated as an alternative to the metal/semiconductor (MS) contacts as their parameters can be varied by using different interlayers. With the aim of determination and control of the parameters of these devices, extensive investigations have been carried out by using different type of organic and inorganic materials as an interlayer (Basman et al. 2015, 2016; Al-Douri et al. 2016; Ibraheam et al. 2016, 2017; Singh et al. 2017; Abd et al. 2013; Ramizy et al. 2011; Omar et al. 2011; Gullu and Turut 2009). However, the usage of DLC films remains limited (Basman et al. 2015). In those limited studies, DLC films were deposited by using either CVD or PVD methods. Furthermore, few of these works investigated diode parameters, such as barrier height ($\phi_b$), ideality factor ($n$) and series resistance ($R_s$) (Gupta et al. 2010; Basman et al. 2015). In a recent study, we have used the electrodeposition technique to obtain a DLC film on Si substrate and then fabricated a MIS diode having showed good rectification ratio with high barrier height (Basman et al. 2015).

This study has two main objective; (1) electrodeposition of Si doped DLC film and investigate its morphological, structural and compositional properties, (2) fabrication of metal–interlayer–semiconductor Schottky diode using the Si–DLC nanocomposite film as an interlayer and investigating its electronic properties. The film was deposited using methanol ($CH_3OH$) as carbon source and tetraethoxysilane ($Si(OC_2H_5)_4$) as Si source. Morphological, structural and compositional properties of the film were investigated by SEM, Raman and XPS analyses, respectively. An Ag/Si–DLC/*p*-Si MIS Schottky diode was fabricated. Electrical characterization of this diode was made by current–voltage (*I–V*) measurements. The ideality factor and barrier height of the MIS diode were calculated by *I–V* and Cheung–Cheung methods.

## 2 Experimental

Electrochemical deposition technique is used to deposit silicon doped diamond-like carbon (Si–DLC) nanocomposite film. The schematic representation of deposition setup can be found elsewhere (Yan et al. 2004c). The deposition of nanocomposite film was carried out by the electrolysis of a mixture of 80 ml analytically methanol ($CH_3OH$; Sigma Aldrich) (N 99.5%) and 400 µl tetraethoxysilane ($Si(OC_2H_5)_4$; Sigma Aldrich) at the applied voltage of 180 V. A *p*-type silicon (100) substrate with resistivity of around 1–10 Ω cm was mounted on the negative electrode, and the counter electrode was graphite plate. The distance between two electrodes was ~ 7 mm. Before the deposition, the silicon substrate was firstly immersed in 5% HF solution to remove the native oxide layer, subsequently ultrasonically cleaned in ethanol and deionized water, and then placed into the electrolyte. Scanning electron microscopy (SEM) images were recorded to observe the morphology of the film using FEI FEG Quanta 450 model SEM operated at 6 kV in secondary electron mode. The Raman spectrum of the film was recorded using a Renishaw spectrometer. The sample was excited with an argon ion laser, operating at 514.5 nm and 25 mW, at room temperature. XPS analysis was performed using a SPECS X-ray photoelectron spectrometer equipped with a monochromatic Al Kα X-ray source (1486.74 eV, 350 W) and a PHOIBOS-100 hemispherical energy analyzer with a MCD5 detector. For metal–interlayer–semiconductor (Ag/Si–DLC/*p*-Si) Schottky diode, Ag contact dot was thermally evaporated on the Si–DLC nanocomposite film with a diameter of 1.0 mm. Ag metal was chosen due to its highest metal work function. Ohmic contact on the backside of the *p*-Si substrate was formed by evaporating of aluminum. All evaporation processes were carried out at about $10^{-6}$ mbar. The schematic structure of the MIS diodes can be found elsewhere (Gullu and Turut 2010). The current–voltage (*I–V*) measurement of the diode was carried out under dark conditions using a source-meter (Keithley 2401).

## 3 Results and discussions

Deposition of Si doped DLC film was achieved at 180 V which is too low when compared with DLC films obtained from methanol (Yan et al. 2004b). Surface morphology of the film was investigated by scanning electron microscope (SEM). SEM images of the Si–DLC film are shown in

Fig. 1. As can be seen, the film showed continuous surface with numerous lumps spread randomly.

We used Raman spectroscopy as an effective technique to investigate the chemical structure of carbon-based materials. In Fig. 2, Raman spectrum of Si-DLC film is shown where the intense peak is appeared at 521 $cm^{-1}$ due to the first order of Si substrate. There is also another broad peak between 880 and 1040 $cm^{-1}$. In that range, both SiC and Si-second order show resonance. Therefore, it was deconvoluted, and two peaks were obtained at 947.8 and 978.7 $cm^{-1}$ (data not shown). These peaks were attributed to Si second-order and SiC, respectively (Bianconi et al. 2004; Ferrari 2002). DLC films show two typical peaks called D and G bands at around 1350 and 1580 $cm^{-1}$, respectively. However, these peaks were not observed in our film because of the abundance of Si–C bonds. The existence of Si–C bonds weakens the effect of C–C bonds. Additionally, increasing level of the disorder also weakens the C–C bonds (Papakonstantinou et al. 2002). In our case, we conclude that Si doping decreases the $sp^2$ clusters and increases $sp^3$ bonds in the film, which is considered as the reason of disappearance of D and G bands. The abundance of $sp^3$ bonds and weaken of $sp^2$ bonds was confirmed by X-ray photoelectron spectroscopy (XPS) analysis. The increment of $sp^3$ bonds is related to Si valance structure. It is well known that carbon and silicon form only four-fold co-ordinated networks (Si–C) (Choi et al. 2007; Papakonstantinou et al. 2002).

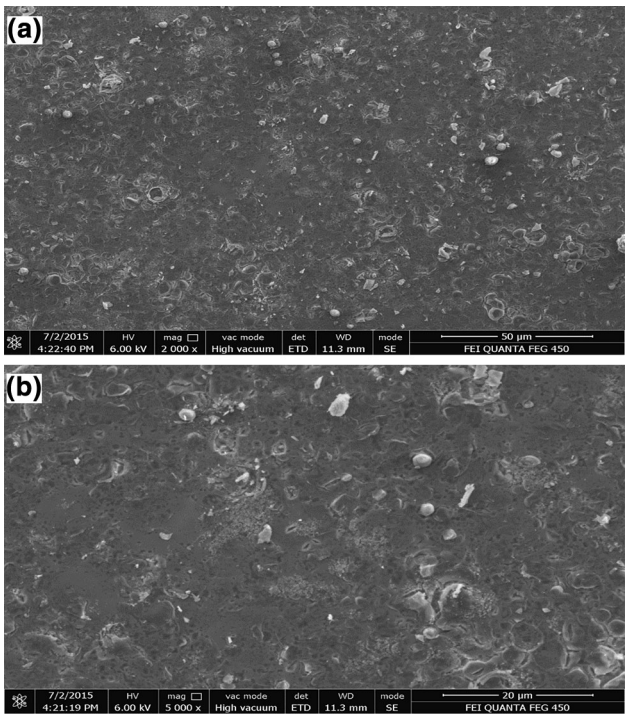



**Fig. 1** SEM images of Si–DLC nanocomposite film

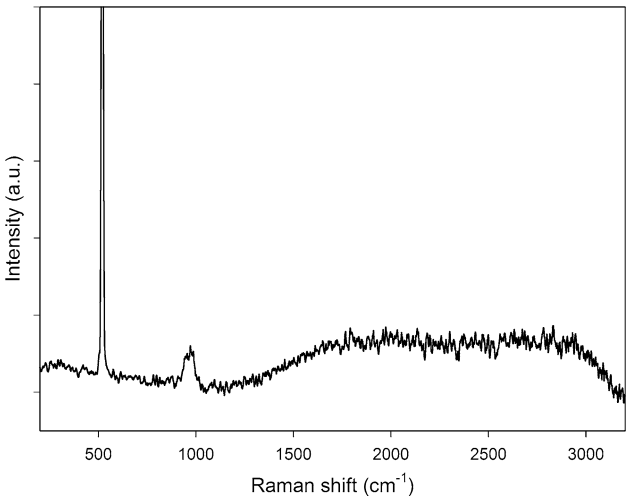



**Fig. 2** Raman spectrum of Si–DLC nanocomposite film

We used XPS to investigate the chemical composition of the film as a common and sensitive technique. The XPS scan survey of Si–DLC film is shown in Fig. 3a. The figure clearly indicates the contributions from C, O and Si. The ratios of Si/C, Si/O and O/C were measured as 0.44, 0.39 and 1.12, respectively. To identify chemical state of the elements, detailed surveys were also carried out. Figure 3b–d show deconvoluted spectra of C 1s, Si 2p and O 1s respectively. Figure 3b demonstrates that C 1s peak is composed of four peaks corresponding C–Si, C–C, C–OH and C=O bonding configurations. Due to high Si concentration which promotes $sp^3$ bonds, the C 1s peak is sharp and mainly indicates C–C bonds in the film. The Si 2p photoelectron spectrum exhibited a broadened peak (Fig. 3c). This peak is composed of five peaks corresponding Si–Si, Si–C, $SiO_4$, and $SiO_2$. Similarly, O 1s spectra was also deconvoluted and it was seen that it is composed of three peaks corresponding to O-metal, C=O or OH and $SiO_2$. XPS spectra imply that $SiO_x$, SiC, C–C, and C–O bonds are the main bonds in the film. Yan et al. (2004b) are the only research group who used the electrochemical method in order to synthesize Si doped DLC composite film. They used dimethylethoxydisilane for doping and obtained DLC film containing polycrystalline $SiO_2$ nanoparticles embedded within an amorphous matrix. In our case, the film exhibited more complex structure. On the other hand, it should be noted that high concentration of tetraethoxysilane promoted the film deposition. We tried to deposit the same film at 200 µl concentration of tetraethoxysilane. The resulted film was uncontinuous and the deposition process took long time.

The experimental semi-logarithmic current–voltage (*I–V*) characteristic of the Ag/Si–DLC/*p*-Si MIS Schottky diode was obtained at room temperature as seen in Fig. 4. The structure exhibits a very good rectifier character

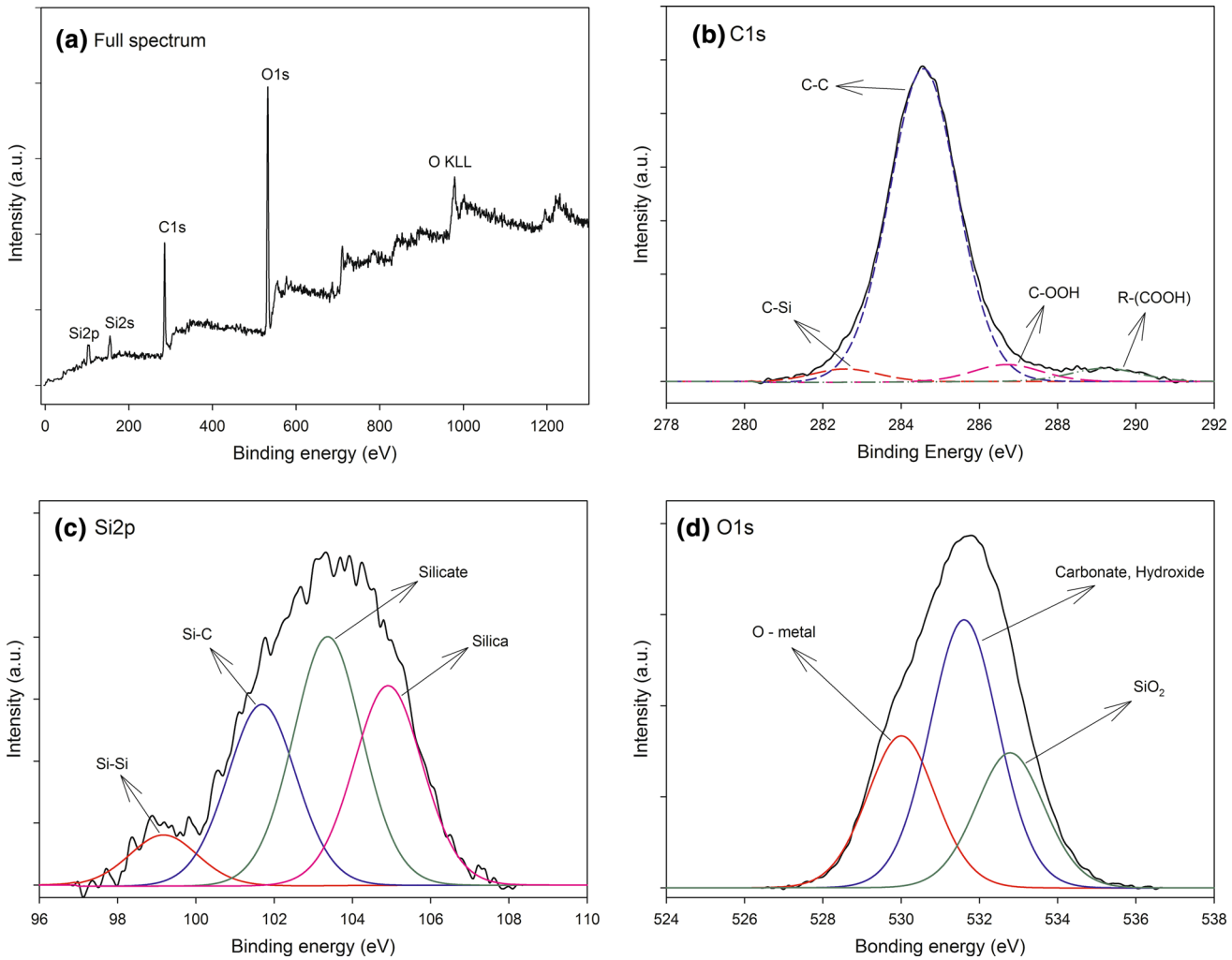



**Fig. 3** XPS survey of Si–DLC nanocomposite film; full spectrum (**a**), and deconvoluted spectra C1s (**b**), Si2p (**c**), O1s (**d**)

(rectification ratio $\sim 10^3$), such that the voltage dependence of current is weak at reverse bias while it increases exponentially at forward bias. Another prominent point of the figure is that the forward bias of the *ln I–V* characteristic displayed two separate linear regions with different slopes in the low bias ($0.08 < V < 0.35$) and intermediate bias ($0.35 < V < 1.5$) regions. These linear regions are indicated by fitting a straight line in Fig. 4. However, this linearity disappears at sufficiently high bias voltages due to the effects of series resistance of contact wires or bulk resistance of the semiconductor and the interfacial layer (Gullu and Turut 2009, 2010; Basman et al. 2012).

In the literature, this type of *I–V* characteristic with two linearity is modeled with two parallel diode model indicating two separate barrier heights (Alialy et al. 2013; Demirezen et al. 2013). Figure 5 shows the equivalent circuit for two parallel diodes model. In this model the current is given by the following equation:

$$I = I_{01}\left[exp\left(\frac{q(V - IR_s)}{n_1 kT}\right) - 1\right] + I_{02}\left[exp\left(\frac{q(V - IR_s)}{n_2 kT}\right) - 1\right] + \left(\frac{V - IR_s}{R_{sh}}\right) \quad (1)$$

where $I_{01}$ and $I_{02}$ are the reverse saturation currents and $n_1$ and $n_2$ are the diode ideality factors. By using Eq. (1), the values of $I_0$, $n$ and $\phi_b$ for Ag/Si–DLC/*p*-Si MIS diode were obtained and presented in Table 1 (for calculation details see: Alialy et al. 2013; Demirezen et al. 2013). As can be seen, both $n_1$ and $n_2$ are higher than unity. For an ideal diode, ideality factor should be close to unity; but for real diodes it is usually higher than one as obtained. The interface state density distribution, quantum–mechanical tunneling, the leakage current, series and shunt resistance etc., are proposed to explain the deviation from unity (Gullu and Turut 2010; Abd et al. 2013; Basman et al. 2016; Monch 1999; Sze 1981). High $n$ values for DLC based MIS structures were also found by Staryga and Bak

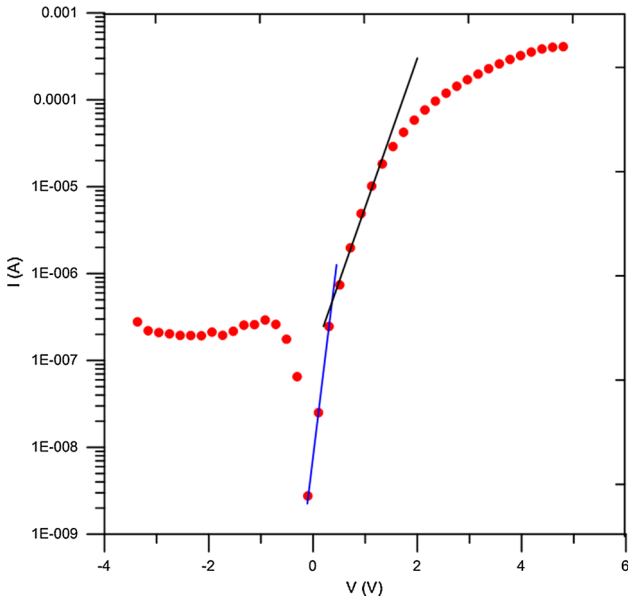



**Fig. 4** The semi-logarithmic I–V plot of the Ag/Si–DLC/*p*-Si MIS diode

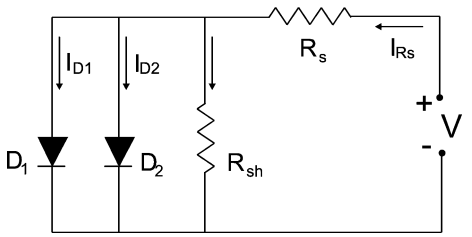



**Fig. 5** The equivalent circuit for two parallel diodes models

(2005) and attributed to hopping transport of charge carriers among localized states. $n_2$ is much higher than $n_1$, i.e., $n$ values depend on the applied voltage. On the other hand, at the intermediate bias, the barrier to electrons gets reduced. The barrier height value change from 0.74 eV at low bias to 0.67 eV at intermediate bias. Shifting values of $n$ and $\phi_b$ indicate different mechanism of conduction in the two linear regions. The results suggest that at low bias the conduction is dominated with hopping of charge carriers among localized states in a narrow band of states (Staryga and Bak 2005). However, in the case of intermediate bias range hopping of charge carriers between bands of localized states occurs. Field dependence conductivity was also observed by other authors for DLC films (Katsuno et al. 2006). In our case the obtained DLC/Si structure behaves like typical MIS structure as conduction depends on the applied voltage (Staryga and Bak 2005).

In the *I–V* plot, the curvatures observed in the high bias voltages are originated from the series resistance effect. As seen from Fig. 5, the diode performance is closely related to series resistance ($R_s$) and shunt resistance ($R_{sh}$) (Alialy et al. 2013; Demirezen et al. 2013; Ramizy et al. 2011). Thus, the determination of these parameters deserves more attention. These values were calculated from the *(dV/dI)–V* plot given in Fig. 6. $R_i$ values converge to a pair of constant values corresponding to $R_s$ and $R_{sh}$, respectively, at both limits of the forward and reverse bias regions. The obtained $R_s$ and $R_{sh}$ values were 6.7 and 25 MΩ, respectively. Regarding these obtained values, it can be clearly seen that both $R_s$ and $R_{sh}$ highly depend on the applied voltage.

The width of linear region of the *ln I–V* plot becomes narrow when $R_s$ value is high enough. In this case, the used *I–V* method for the calculation of ideality factor $n$ and barrier height $\phi_b$ values becomes unreliable. Cheung and Cheung (1986) developed a method in which series resistance $R_s$, ideality factor $n$ and barrier height $\phi_b$ can be also calculated from the high forward bias region of *ln I–V* plot (Gullu and Turut 2009; Cheung and Cheung 1986). According to Cheung and Cheung (1986), these parameters can be determined from the following equations:

$$\frac{dV}{dln(I)} = IR_S - n\left(\frac{kT}{q}\right) \tag{2}$$

$$H(I) = V - n\left(\frac{kT}{q}\right) ln\left(\frac{I}{AA^*T^2}\right) \tag{3}$$

$$H(I) = IR_S + n\phi_b \tag{4}$$

Details on the determination of $n$, $\phi_b$ and $R_s$ values using Cheung–Cheung method can be found elsewhere (Cheung and Cheung 1986; Basman et al. 2012). The plot of $dV/d(\ln I)-I$ yields a straight line for the curvature in the high bias region (Fig. 7a). According to Eq. (3), the slope of this line gives $R_s$ whereas the interception point of $dV/d(\ln I)$ axis with the line gives $nkT/q$. Hereby, $n$ and $R_s$ were calculated as 16.99 and 5.17 kΩ, respectively. On the other hand, the slope of the $H(I) - I$ plot (Fig. 7b) drawn according to Eq. (4) yields a second $R_S$ value. Also, at the same plot, the interception point of the $H(I)$ axis equals to

**Table 1** The calculated diode parameters of the Ag/Si–DLC/*p*-Si MIS Schottky diode from *I–V*, Cheung–Cheung methods

| Diode parameters | *I–V* method | | Cheung–Cheung method | |
|---|---|---|---|---|
| | I. Linear region | II. Linear region | $\frac{dV}{d(\ln I)} - I$ | $H(I) - I$ |
| Ideality factor ($n$) | 3.42 | 9.79 | 16.99 | |
| Barrier height ($\phi_b$; eV) | 0.74 | 0.67 | | 0.61 |
| Series resistance ($R_s$; kΩ) | – | – | 5.17 | 4.76 |

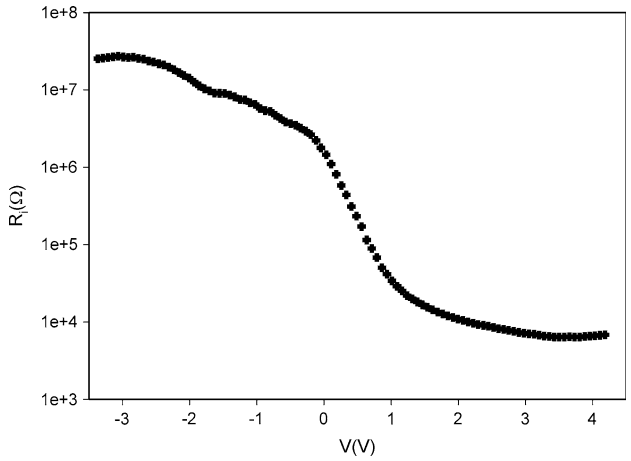



**Fig. 6** The plot of the voltage dependent resistance of the Ag/Si–DLC/*p*-Si MIS diode

$n\phi_b$. Accordingly, the obtained values of $\phi_b$ and $R_S$ are 0.61 eV and 4.76 kΩ, respectively. The $R_S$ values obtained from Cheung–Cheung method are close to each other. The differences between the ideality factors and barrier heights calculated using *I–V* and Cheung–Cheung method are due to the fact that these two use different regions of the *ln*(*I*)–*V* graph for calculation. To calculate electrical parameters of the diode, the *I–V* method utilizes the linear region neglecting the series resistance, while Cheung–Cheung method uses the nonlinear region in which interfacial layer thickness and series resistance are effective (Aydogan et al. 2009).

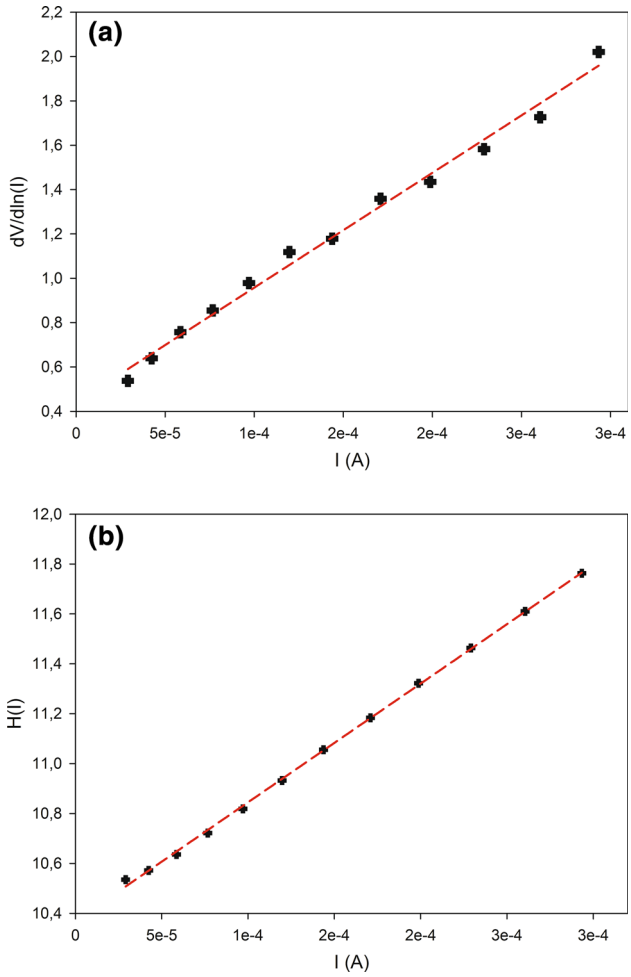



**Fig. 7** The Plots of *dV/d*(*InI*) vs. *I* (**a**) and *H*(*I*) vs. *I* (**b**) obtained from forward bias I–V data given in Fig. 4

## 4 Conclusions

In this study, silicon doped DLC nanocomposite film has been successfully deposited on *p*-type silicon substrate via electrodeposition at low voltage. The morphology and structure of the film were investigated and then the film was used as an interlayer to fabricate an Ag/Si–DLC/*p*-Si MIS Schottky diode. The electrical characteristics of the device was analyzed by *I–V* measurements. Based on the analyses, the following conclusions can be drawn:

- The film showed continuous surface with numerous lumps spread randomly.
- Typical D and G bands of DLC films were not observed in the Raman spectrum due to abundance of Si–C bonds.
- Silicon incorporation promoted the film deposition and increased $sp^3$ bonds in the film
- The fabricated Ag/Si–DLC/*p*-Si MIS Shocttky diode exhibited good rectifier character with $\sim 10^3$ rectification ratio.
- In the forward bias semi-logarithmic *I–V* plot, two linear regions with different slopes were observed. Such behavior was modelled by two parallel diodes and attributed to different conduction mechanism.
- The main electrical parameters, such as barrier height, ideality factor and series resistance were calculated by *I–V* and Cheung–Cheung methods.
- The Si–DLC nanocomposite film acted as barrier height modifier in the MIS diode.

**Acknowledgements** This work was supported by the Scientific Research Project Committee of Gaziosmanpasa University (under the Grand contract no: 2015/88).

## References

Abd HR, Al-Douri Y, Ahmed NM, Hashim U (2013) Alternative-current electrochemical etching of uniform porous silicon for photodetector applications. Int J Electrochem Sci 8:11461–11473

Ahmed SF, Moon MW, Lee KR (2009) Effect of silver doping on optical property of diamond like carbon films. Thin Solid Films 517:4035–4038

Al-Douri Y, Ameri M, Bouhemadou A, Khenata R (2016) Annealing temperature effect on structural, optical, morphological and electrical properties of CdS/Si(100) nanostructures. Microsyst Technol 22(10):2529–2541

Alialy S, Tecimer H, Uslu H, Altındal S (2013) A comparative study on electrical characteristics of Au/N-Si Schottky diodes, with and without bi-doped pva interfacial layer in dark and under illumination at room temperature. J Nanomed Nanotechol 4(3):1000167

Aydogan S, Saglam M, Turut A, Onganer Y (2009) Series resistance determination of Au/polypyrrole/p-Si/Al structure by current–voltage measurements at low temperatures. Mater Sci Eng C 29(4):1486–1490

Basman N, Uzun O, Fiat S, Alkan C, Cankaya G (2012) Electrical characterization of a pre-ceramic polymer modified Ag/poly(hydridocarbyne)/p-Si Schottky barrier diode. J Mater Sci Mater Electron 23(12):2282–2288

Basman N, Aslan N, Uzun O, Cankaya G, Kolemen U (2015) Electrical characterization of metal/diamond-like carbon/inorganic semiconductor MIS Schottky barrier diodes. Microelectron Eng 140:18–22

Basman N, Uzun R, Ozcakır R, Erol I, Cankaya G, Uzun O (2016) Effect of a new methacrylic monomer on diode parameters of Ag/p-Si Schottky contact. J Microelectron Electron Compon Mater 46:190–196

Bhattacharyya S, Silva SRP (2007) Demonstration of an amorphous carbon tunnel diode. Appl Phys Lett 90(8):082105

Bianconi PA, Joray SJ, Aldrich BL, Sumranjit J, Duffy DJ, Long DP, Lazorcik JL, Raboin L, Kearns JK, Smulligan SL, Babyak JM (2004) Diamond and diamond-like carbon from a preceramic polymer. J Am Chem Soc 126(10):3191–3202

Caschera D, Federici F, Pandolfi L, Kaciulis S, Sebastiani M, Bemporad E, Padeletti G (2011) Effect of composition on mechanical behaviour of diamond-like carbon coatings modified with titanium. Thin Solid Films 519:3061–3067

Chaus AS, Fedosenko TN, Rogachev AV, Čaplovič Ľ (2014) Surface, microstructure and optical properties of copper-doped diamond-like carbon coating deposited in pulsed cathodic arc plasma. Diam Relat Mater 42:64–70

Cheung SK, Cheung NW (1986) Extraction of Schottky diode parameters from forward current–voltage characteristics. Appl Phys Lett 49(2):85–87

Choi J, Kawaguchi M, Kato T, Ikeyama M (2007) Deposition of Si–DLC film and its microstructural, tribological and corrosion properties. Microsyst Technol 13:1353–1358

Demirezen S, Altındal S, Uslu I (2013) Two diodes model and illumination effect on the forward and reverse bias I–V and C–V characteristics of Au/PVA (bi-doped)/n-Si photodiode at room temperature. Curr Appl Phys 13:53–59

Erdemir A, Donnet C (2006) Tribology of diamond-like carbon films: recent progress and future prospects. J Phys D Appl Phys 39(18):311–327

Ferrari AC (2002) Determination of bonding in diamond-like carbon by Raman spectrocopy. Diam Relat Mater 11:1053–1061

Franta D, Ohlidal I, Bursikova V, Zajickova L (2003) Optical properties of diamond-like carbon films containing $SiO_x$. Diam Relat Mater 12:1532–1538

Gao X, Xue Q, Hao L, Zheng Q, Li Q (2007) Ammonia sensitivity of amorphous carbon film/silicon heterojunctions. Appl Phys Lett 91(12):122110

Guerino M, Massi M, Maciel HS, Otani C, Mansano RD (2003) The effects of the nitrogen on the electrical and structural properties of the diamond-like carbon (DLC) films. Microelectron J 34:639–641

Gullu O, Turut A (2009) Electrical analysis of organic interlayer based metal/interlayer/semiconductor diode structures. J Appl Phys 106(10):103717

Gullu O, Turut A (2010) Electrical analysis of organic dye-based MIS Schottky contacts. Microelectron Eng 87(12):2482–2487

Gupta RK, Ghosh K, Kahol PK (2010) Current-voltage characteristics of p-Si/carbon junctions fabricated by pulsed laser deposition. Microelectron Eng 87(2):221–224

Huang L, Jiang H, Zhang J, Zhang Z, Zhang P (2006) Synthesis of copper nanoparticles containing diamond-like carbon films by electrochemical method. Electrochem Commun 8:262–266

Ibraheam AS, Al-Douri Y, Al-Fhdawi JMS, Al-Jumaili HS, Verma KD, Hashim U, Ayub RM, Ruslinda AR, Md Arshad MK, Reshak AH, Abd Hamid SB (2016) Structural, optical and electrical properties of $Cu_2Zn_{1-x}Cd_xSnS_4$ quinternary alloys Nanostructures deposited on porous silicon. Microsyst Technol 22:2893–2900

Ibraheam AS, Al-Douri Y, Hashim U, Ameri M, Bouhemadou A, Khenata R (2017) Structural, optical and electrical investigations of $Cu_2Zn_{1-x}Cd_xSnS_4$/Si quinternary alloy nanostructures synthesized by spin coating technique. Microsyst Technol 23(6):2223–2232

Katsuno T, Godet C, Loir AS, Garrélie F (2006) Hopping current density in amorphous carbon/crystalline silicon heterojunctions. J Noncryst Solids 352:1421–1424

Kima HG, Ahna SH, Kima JG, Parkb SJ, Lee KR (2005) Effect of Si-incorporation on wear-corrosion properties of diamond-like carbon films. Thin Solid Films 482:299–304

Laurikaitienė J, Meškinis Š, Adlienė D, Šablinskas V, Tamulevičius S, Kopustinskas V, Šniurevičiūtė M, Mockevičienė S, Gudaitis R (2008) Electrical properties of the diamond like carbon films irradiated with high energy photons. J Phys Conf Ser 100:072036

Li RS, Liu B, Zhou M, Zhang ZX, Wang T, Lu BA, Xie EQ (2009) Effect of deposition voltage on the field emission properties of electrodeposited diamond-like carbon films. Appl Surf Sci 255(9):4754–4757

Meškinis Š, Vasiliauskas A, Šlapikas K, Gudaitis R, Andrulevičius M, Čiegis A, Niaura G, Kondrotas R, Tamulevičius S (2014) Bias effects on structure and piezoresistive properties of DLC: Ag thin films. Surf Coat Technol 255:84–89

Milne WI (2003) Electronic devices from diamond-like carbon. Semicond Sci Technol 18:81–85

Monch W (1999) Barrier heights of real Schottky contacts explained by metal-induced gap states and lateral inhomogeneities. J Vac Sci Technol B 17(4):1867

Nery RPOS, Bonelli RS, Camargo SS Jr (2010) Evaluation of corrosion resistance of diamond-like carbon films deposited onto AISI 4340 steel. J Mater Sci 45(20):5472–5477

Omar K, Al-Douri Y, Ramizy A, Hassan Z (2011) Stiffness properties of porous silicon nanowires fabricated by electrochemical and laser-induced etching. Superlattices Microstruct 50:119–127

Papakonstantinou P, Zhao JF, Lemoine P, McAdams ET, McLaughlin JA (2002) The effects of Si incorporation on the electrochemical and nanomechanical properties of DLC thin films. Diam Relat Mater 11:1074–1080

Ramizy A, Hassan Z, Omar K, Al-Douri Y, Mahdi MA (2011) New optical features to enhance solar cell performance based on porous silicon surfaces. Appl Surf Sci 257:6112–6117

Robertson J (2002) Diamond-like carbon. Mater Sci Eng R 37:129–281

Silva SRP, Amaratunga GAJ, Okano K (1999) Modeling of the electron field emission process in polycrystalline diamond and diamond-like carbon thin films. J Vac Sci Technol B 17(2):557–561

Singh S, Dillip GR, Vyas S, Hasan MdR, Park IK, Chakrabarti P, Park SH (2017) Fabrication and characterization of hydrothermally grown MgZnO nanorod films for Schottky diode applications. Microsyst Technol 23(1):39–46

Staryga E, Bak GW (2005) Relation between physical structure and electrical properties of diamond-like carbon thin films. Diam Relat Mater 14:23–34

Sze SM (1981) Physics of semiconductor devices, 2nd edn. Wiley, New York

Tao Y, Yi D, Zhu B, Wang D, Wang Z, He K (2011) Direct hydrothermal electrochemical preparation of diamond-like carbon films on substrates. J Mater Sci 46(4):1136–1138

Wan S, Wang L, Xue Q (2010) Electrochemical deposition of sulfur doped DLC nanocomposite film at atmospheric pressure. Electrochem Commun 12(1):61–65

Wang FM, Chen MW, Lai QB (2010) Metallic contacts to nitrogen and boron doped diamond-like carbon films. Thin Solid Films 518(12):3332–3336

Yan X, Xu T, Chen G, Liu HW, Yang SR (2004a) Effect of deposition voltage on the microstructure of electrochemically deposited hydrogenated amorphous carbon films. Carbon 42(15):3103–3108

Yan X, Xu T, Chen G, Xue Q, Yang S (2004b) Synthesis of diamond-like carbon/nanosilica composite films by an electrochemical method. Electrochem Commun 6:1159–1162

Yan X, Xu T, Chen G, Yang S, Liu H (2004c) Study of structure, tribological properties and growth mechanism of DLC and nitrogen-doped DLC films deposited by electrochemical technique. Appl Surf Sci 236:328–335

Yi JW, Kim JK, Moon MW, Lee KR, Kim SS (2009) Tribological performance of alternating-layered Si–DLC/DLC films under humid conditions. Tribol Lett 34:223–228

Zeng A, Neto VF, Gracio JJ, Fan QH (2014) Diamond-like carbon (DLC) films as electrochemical electrodes. Diam Relat Mater 43:12–22

Zhang J, Huang L, Yu L, Zhang P (2008) Synthesis and tribological behaviors of diamond-like carbon films by electrodeposition from solution of acetonitrile and water. Appl Surf Sci 254(13):3896–3901